The Design and Development of a Logarithmic-Shaped Soft Gripper

Halil Hulusi Hoşgör, and Zafer Bingül
Department of Mechatronics Engineering
Kocaeli University
Kocaeli, Türkiye
216113001@kocaeli.edu.tr, zaferb@kocaeli.edu.tr

***Abstract*— Soft robotic systems have attracted considerable research interest owing to their promising potential in specialized and unstructured applications. This study presents the design and development of a logarithmic spiral-shaped soft gripper. The forward kinematic formulations required for fabrication were systematically derived, and key design parameters, dynamics, workspace characteristics, and simulation methodologies were thoroughly investigated. The gripper was developed in a segmented configuration inspired by an *n*-pendulum structure, facilitating the efficient kinematic analysis of compliant designs that are inherently challenging to model and simulate. Furthermore, a comprehensive review of the existing literature on soft grippers incorporating logarithmic spiral geometries was conducted. The outcomes of this study provide a foundational framework for the future design, optimization, and implementation of logarithmic spiral-shaped soft grippers.**

Keywords—logarithmic spiral, soft gripper, human–machine interaction, forward kinematics, dynamics, workspace, simulation.

I. Introduction

Soft robots are inherently flexible, jointless systems with virtually unlimited degrees of freedom, typically fabricated using rapid prototyping techniques or by casting silicone-based elastomeric materials into custom molds. Compared with conventional rigid-body robots, soft robotic systems offer notable advantages in terms of reduced weight, lower cost, mechanical compliance, and adaptability. Nevertheless, their control remains a significant challenge, and their positioning accuracy and operational speed are generally inferior to those of conventional robotic systems. As a result, soft robots are not yet capable of achieving the performance levels of serial manipulators in tasks demanding high precision. Owing to their compliant and deformable structures, however, soft robots exhibit a remarkable ability to adapt to environmental constraints. Furthermore, their inherent mechanical compliance substantially reduces the need for precise motion programming.

Soft robots are widely inspired by biological systems and are used in applications such as safe human–machine interaction, agricultural automation, medical and rehabilitation systems, and the manipulation of delicate or fragile objects. Several biological structures exhibit characteristic logarithmic spiral geometries, including the seahorse tail, elephant trunk, gastropod shells, octopus arms, chameleon tail, and spider webs. Beyond biological systems, natural phenomena such as the spatial distribution of galaxies and the rotational patterns observed in hurricane satellite imagery also exhibit logarithmic spiral configurations, as illustrated in Fig. 1.

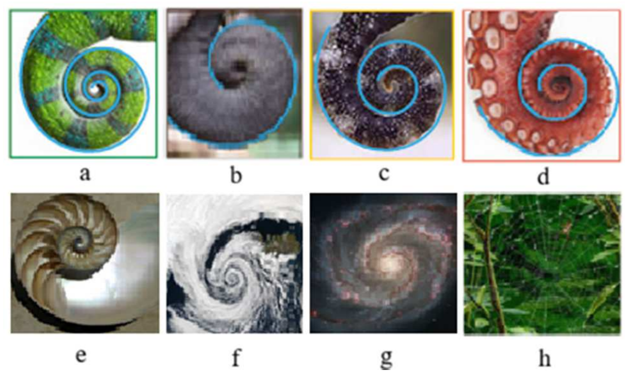

Fig. 1. Examples of natural structures and phenomena exhibiting logarithmic spiral characteristics: (a) chameleon tail, (b) elephant trunk, (c) seahorse tail, (d) octopus arm, (e) gastropod shell, (f) hurricane, (g) galaxy, (h) spider web.

Research on soft grippers has increased substantially since 2002, reflecting the growing interest in compliant robotic systems. These studies can be broadly categorized according to actuator type, kinematic and dynamic modeling approaches, and control strategies.

Rahn developed a cable-driven continuum robot in which nonlinear kinematic formulations were derived for a single segment and subsequently extended to all segments of the design. Displacement, load capacity, and optimal cable carrier design were systematically evaluated [1]. McMahan presented an octopus-arm-inspired soft manipulator, with real-time implementation realized through MATLAB/Simulink software and a remote-control interface [2]. Mazzolai modeled an octopus arm incorporating a shape memory alloy (SMA) spring, and the temperature-dependent workspace of the design was analyzed [3]. Deng designed and implemented a cable-driven soft robot intended for cardiac surgical applications [4]. A soft gripper inspired by octopus tentacles was developed, comprising three soft fingers and twelve cables. The dynamic model of the system was derived, and both curvilinear and linear workspaces were characterized [5]. A subsequent study employed stepper-motor-controlled cables in conjunction with shape memory polymer joints exhibiting temperature-dependent stiffness, with Gaussian modeling performed under an open-loop control scheme [6]. An elastomeric microtube-based pneumatic soft actuator was additionally developed [7]. A hydraulically amplified selfhealing electrostatic actuator with muscle-like performance was proposed, drawing inspiration from the versatility of the elephant trunk [8]. An octopus-arm-inspired gripper incorporating a vacuum-actuated suction mechanism was investigated, demonstrating enhanced gripping capacity [9]. A novel soft pneumatic actuator (SPA) featuring a spiral configuration was proposed, inspired by the structural properties of the seahorse tail [10]. A cable-driven continuum robot with tapered tensegrity was presented, inspired by the high adaptability of seahorse tails, enabling conformal grasping of objects with varying curvatures. A static model based on geometric relationships and the virtual work principle was formulated in that study [11]. A soft pneumatic actuator was developed and evaluated through simulations, parametric optimizations, and dynamic finite element analyses conducted in Abaqus [12]. A novel hybrid rigid-soft continuum manipulator was introduced, designed using Euler–Bernoulli beam theory and geometric inference, with compliance, adaptability, and tactile sensing capabilities demonstrated experimentally [13]. A spiral-shaped flexible mechanism intended for body weight support was additionally proposed, with parametric and geometric analyses carried out [14]. Lifelike motion and stable grasping were achieved through simple cable-driven actuation by means of soft robots replicating the logarithmic spiral, a pattern observed throughout nature [15].

II. Materials And Methods

A. Logarithmic Spiral

A logarithmic spiral, also referred to as an equiangular spiral or growth spiral, was first studied in the 17th century by René Descartes and Jakob Bernoulli. Due to its remarkable mathematical properties, Bernoulli named this curve *spira mirabilis* (the miraculous spiral).

The logarithmic spiral is geometrically distinct from the Archimedean spiral in that the radial distance between successive turns increases progressively, whereas in the Archimedean spiral this spacing remains constant, as illustrated in Fig. 2 [16].

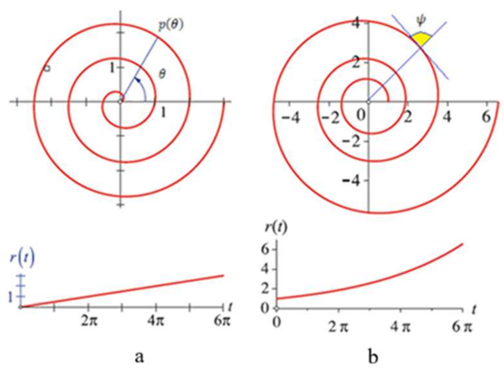

Fig. 2. Comparison of spiral geometries: (a) Archimedean spiral and (b) logarithmic spiral.

The logarithmic spiral is expressed in polar coordinates in Equation (1).

$$p(\theta) = ae^{b\theta} = e^{b\left(\frac{\ln a}{b}+\theta\right)} \quad (1)$$

where a and b are scaling parameters, and b represents the cotangent of the constant polar tangential angle ψ ($b = \cot\psi$), defined as the angle between the tangent at a given point on the spiral and the line connecting that point to the origin. a characterizes the translation in the angular domain and b governs the radial scaling [15].

B. Coordinate System and Design Details

The logarithmic spiral-shaped soft gripper consists of 18 discrete segments. Initially, a single segment was modeled, after which the remaining segments were designed as individual components in SolidWorks using a uniform scaling factor of 0.9125. The system is in its reference configuration when all segments are aligned in parallel and perpendicular orientations. The segment dimensions decrease progressively from the base to the tip at a constant ratio, as uniform discretization is applied in the angular domain, which is essential for the gripper to curl into a logarithmic spiral profile. This approach enables a single unit to be designed and subsequently scaled to obtain grippers of varying sizes. The sequential arrangement and uncurling of these segments naturally yield a tapered structure. Furthermore, a coordinate frame was established at the bottom midpoint of the lowermost segment, as illustrated in Fig. 3.

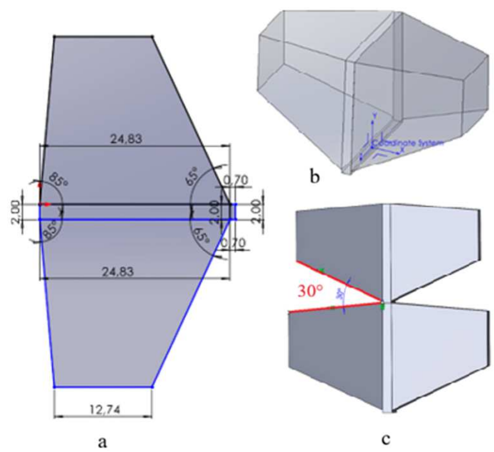

Fig. 3. Design details of the logarithmic spiral-shaped soft gripper: (a) segment dimensions, (b) coordinate frame placement, and (c) joint angle limits.

Fig. 4 illustrates the key design parameters of the soft gripper structure. The parameter φ is defined as the taper angle, characterizing the conical geometry of the gripper. The parameter $\delta(\theta)$ denotes the segment width, while $\sigma(\theta)$ represents the width of the middle layer.

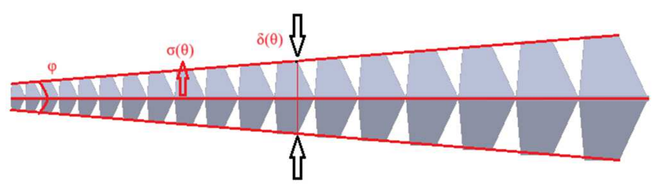

Fig. 4. Key design parameters of the logarithmic spiral-shaped soft gripper.

Upon completing the sketch, the lower, middle, and upper sections are extruded independently with a symmetric depth of 7 mm. A draft angle of 15° is then applied to each section. The design procedure for a single segment is illustrated in Fig. 5.

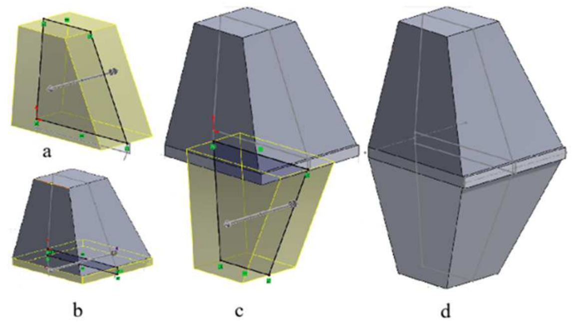

Fig. 5. Single segment design procedure: (a) extrusion of the upper section, (b) extrusion of the middle section, (c) extrusion of the lower section, and (d) final design of a single segment.

C. Forward Kinematic Calculations

Kinematics is the branch of mechanics concerned with the analysis of motion and geometric configurations of systems, independent of the forces responsible for that motion. Forward kinematics addresses the positional, velocity, and acceleration relationships among the links of a robotic system. By applying a sequence of homogeneous transformation matrices, the spatial relationship between the base frame and the end-effector frame can be systematically established. This mathematical formulation is referred to as the forward kinematic model of the robot [17].

The forward kinematics of the designed soft gripper can be determined using two distinct approaches: a geometric method and the Denavit–Hartenberg (DH) parameter method.

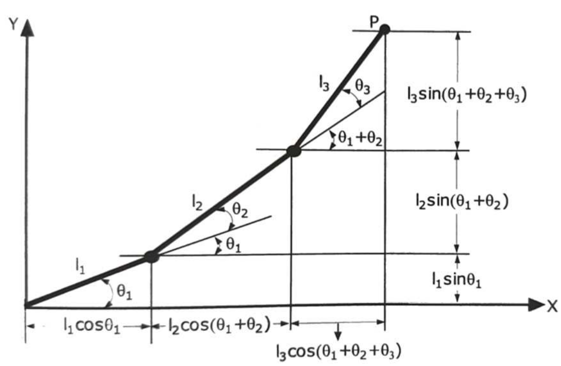

Fig. 6. Forward kinematic analysis of the soft gripper using the geometric approach.

The forward kinematic formulation using the geometric approach is illustrated in Fig. 6. The coordinates of the joint points are determined using Equations (2) and (3), where *I* represents the link length and *θ* denotes the relative angular displacement between consecutive segments.

$$P_x = I_1 \cos\theta_1 + \cdots + I_N \cos(\theta_1 + \cdots + \theta_N) \tag{2}$$

$$P_y = I_1 \sin\theta_1 + \cdots + I_N \sin(\theta_1 + \cdots + \theta_N) \tag{3}$$

The forward kinematics can alternatively be derived using the Denavit–Hartenberg (D–H) parameter method. For a serial manipulator with *n* degrees of freedom, the homogeneous transformation matrix corresponding to the *i*-th joint is obtained as given in Equation (4), where *T* denotes the transformation matrix, *a* represents the link length, *α* is the link twist angle, *d* represents the link offset, and *θ* denotes the joint angle.

$$^{i-1}_{i}T = R_x(\alpha_{i-1}) D_x(a_{i-1}) R_z(\theta_i) D_z(d_i) \tag{4}$$

Applying Equation (4), the homogeneous transformation matrix of an individual joint is obtained, as presented in Equation (5).

$$^{i-1}_{i}T = \begin{bmatrix} \cos\theta_i & -\sin\theta_i & 0 & a_{i-1} \\ \sin\theta_i \cos\alpha_{i-1} & \cos\theta_i \cos\alpha_{i-1} & -\sin\alpha_{i-1} & -\sin\alpha_{i-1} d_i \\ \sin\theta_i \sin\alpha_{i-1} & \cos\theta_i \sin\alpha_{i-1} & \cos\alpha_{i-1} & \cos\alpha_{i-1} d_i \\ 0 & 0 & 0 & 1 \end{bmatrix} \tag{5}$$

The D–H parameters are determined as listed in Table I. The coordinates of the end-effector are subsequently obtained using Equation (6).

$$^{0}_{N}T = {}^{0}_{1}T\,{}^{1}_{2}T\,{}^{2}_{3}T \ldots {}^{N-1}_{N}T \tag{6}$$

TABLE I. THE D-H PARAMETERS FOR TRANSFORMATION MATRIX

No	D-H Parameters				
	α_{i-1}	a_{i-1}	d_i	θ_i	*Variable*
1	0	0	0	θ_1	θ_1
2	0	I_1	0	θ_2	θ_2
3	0	I_2	0	θ_3	θ_3
4	0	I_3	0	θ_4	θ_4
$N-1$	0	I_{N-1}	0	θ_N	θ_N
N	0	I_N	0	0	0

D. Dynamic Calculations

The dynamic analysis of a robotic arm concerns the relationship between the joint torques or forces generated by actuators and the time-dependent position, velocity, and acceleration of the system. Such analyses can be performed using established methods, including the Lagrange–Euler, Newton–Euler, and d'Alembert formulations. The kinetic energy depends on both the configuration and velocity of the system, whereas the potential energy depends only on its configuration [18].

The dynamic equations of the system can be derived using the Lagrange–Euler formulation as follows:

$$L(q,\dot{q}) = K(q,\dot{q}) - P(q) \tag{7}$$

$$K(q,\dot{q}) = \frac{1}{2}(\dot{q})^T D(q)\dot{q} \tag{8}$$

where $\dot{q} = (dq\,/\,dt)$ and $D(q) = \sum_{i=1}^{n}[(A_i)^T m_i A_i + (B_i)^T I_i B_i]$.

$$P(q) = \sum_{i=1}^{n} m_i\, g^T h_i \tag{9}$$

where *K* denotes the kinetic energy, *P* represents the potential energy of the system, *A* denotes the Jacobian matrix of the linear velocities, and *B* represents the Jacobian matrix of the angular velocities. By substituting the derived kinetic and potential energy expressions into Equation (7) and rearranging the terms, the dynamic equation of motion is obtained as shown in Equation (10).

$$L(q,\dot{q}) = \frac{1}{2}(\dot{q})^T D(q)\dot{q} + mg^T h \tag{10}$$

The equation of motion arising from the dynamic behavior of the robotic system is presented in Equation (11).

$$\tau = \frac{d}{dt}\frac{\partial K}{\partial \dot{q}} - \frac{\partial K}{\partial q} + \frac{\partial P}{\partial q} \tag{11}$$

By substituting the kinetic and potential energy expressions into the equation of motion, the dynamic equation of a robotic arm in joint space is expressed as given in Equation (12), where *D* denotes the generalized inertia matrix of the manipulator, *C* represents the Coriolis and centrifugal force vector, *G* denotes the gravitational force vector, and *b* denotes the system friction term.

$$\tau_i = \sum_{i=1}^{n} D_{ij}(q)\ddot{q}_j + \sum_{k=1}^{n}\sum_{j=1}^{n} C_{kj}(q)\dot{q}_k\,\dot{q}_j + G_i(q) + b_i(\dot{q}) \tag{12}$$

E. Design Components and Fabrication

The components designed in SolidWorks were fabricated using a rapid-prototyping-based 3D printer. The part files were exported in STL format and imported into the printer software. White thermoplastic polyurethane (TPU 95A) filament was used asp the fabrication material because its elastic restoring properties allow the gripper to uncurl upon release of the cable tension. The experimental setup is illustrated in Fig. 7.

The gripper structure is actuated by a cable routed along the robot body, with one end fixed to the tip and the other connected to a motor, enabling the structure to curl and wrap around objects.

GM6020 brushless DC motors were selected for gripper actuation. The motor specifications include a no-load speed of 320 rpm, an operating current of 1.62 A, a rated voltage of 24 V DC, a holding torque of 1.2 N·m, and a mass of 468 g.

A RoboMaster development board was employed as the control unit, featuring a 32-bit STM32F407 microcontroller, an operating voltage of 3.3 V, an input voltage range of 6–20 V, six digital input/output pins, seven PWM output channels, 2 CAN bus communication ports, and a clock frequency of 168 MHz.

III. RESULTS AND DISCUSSION

In contrast to existing studies, the design parameters of the proposed gripper were comprehensively presented and analyzed. Moreover, the use of the *n*-joint pendulum approach for kinematic modeling constitutes a distinctive aspect of this work. The control strategies employed in the dynamic analysis and the corresponding results are expected to serve as a reference for future research.

The simulation results demonstrate that the accessible workspace of the gripper increases as the taper angle decreases and decreases as the taper angle increases. Furthermore, the thickness of the middle layer significantly influences the motion characteristics of the gripper: an excessively thin middle layer causes inter-segment collisions, whereas an overly thick layer requires higher actuation force to achieve bending.

The accuracy of the derived forward kinematic formulations was verified through quantitative comparison between simulation results and experimental measurements. Additionally, a compliant design inspired by an *n-point* pendulum structure was successfully realized via a segmented modeling approach. The kinematic simulation was performed by assigning angular values to each joint.

Dynamic analysis was conducted using a sliding mode controller. System responses were obtained based on a predefined trajectory, and the end-effector velocity, position, and position error were evaluated through graphical results. Owing to the compliant structure of the system and the high actuation speed of the motors, the end-effector initially overshoots the target position. The sliding mode controller subsequently stabilizes the system and enables convergence to the desired position within 3 s.

Fig. 7 illustrates the capability of the developed gripper to grasp objects of varying sizes and geometries. The results confirm the adaptability and versatility of the proposed gripper in handling objects with diverse shapes and diameters ranging from 20 mm to 60 mm.

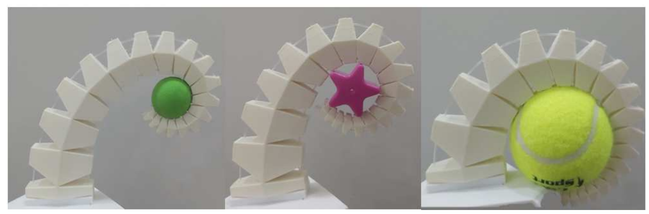

Fig. 7. Experimental setup and demonstration of the logarithmic spiral-shaped soft gripper grasping objects of varying sizes and geometries.

A. Forward Kinematics Application

When the joint angles of the soft gripper were set to θ_1, θ_2, and θ_3, the resulting configurations are illustrated in Fig. 8. The corresponding end-effector positions were plotted.

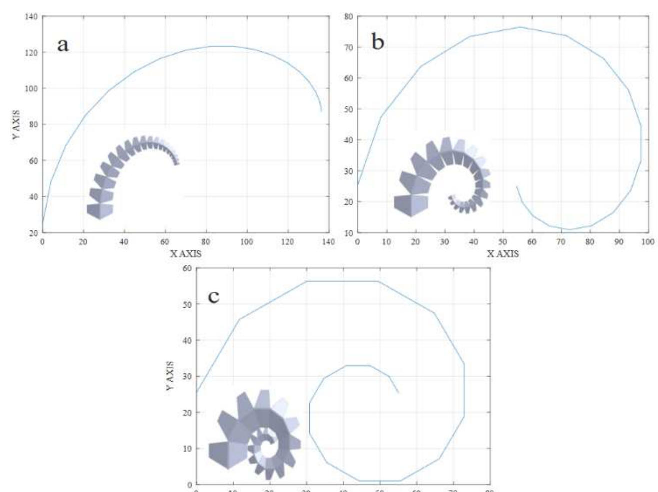

Fig. 8. Configurations of the soft gripper at varying joint angles: (a) $\theta = 10°$, (b) $\theta = 20°$, (c) $\theta = 30°$.

It was verified that the segment positions of the soft gripper obtained in SolidWorks are in exact agreement with those calculated via forward kinematics. Fig. 9 illustrates the end-effector positions computed in MATLAB using the derived forward kinematic model at a uniform joint angle of 30°.

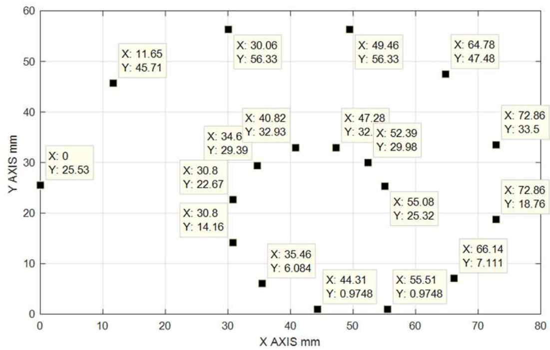

Fig. 9. Segment positions of the soft gripper computed via forward kinematics at a uniform joint angle of 30°.

In SolidWorks, the Angle Mate tool was utilized to obtain reference angle values, and the Reference Geometry tool was employed to define the reference coordinate frame. The positions of each segment of the soft gripper with respect to the established coordinate frame were extracted using the Measure tool, as illustrated in Fig. 10. The positional accuracy of the forward kinematic formulations was subsequently validated against the experimental setup.

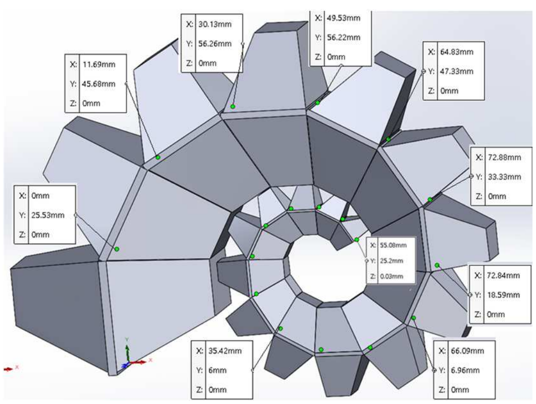

Fig. 10. Segment positions of the designed soft gripper extracted via the SolidWorks Measure tool.

B. Simulation

To enable active control and determine the operational workspace of the system under joint angle limits, kinematic constraints, and inter-link collisions, the SolidWorks model was transferred to Simscape Multibody. The mechanical model was automatically generated in the Simulink environment, as shown in Fig. 11. The model consists of rigid body components and joint angle blocks. Joint angle inputs are converted to radians before being applied to the respective joint blocks.

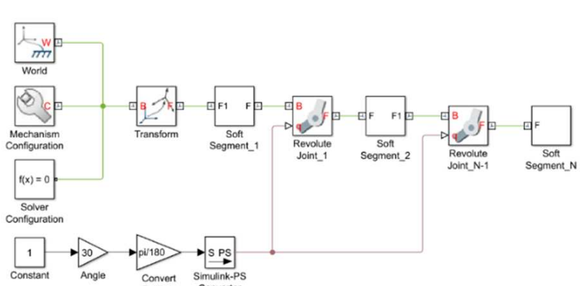

Fig. 11. Simulink model of the logarithmic spiral-shaped soft gripper.

Upon execution of the Simulink model, the Simscape simulation is activated. The system is simulated synchronously based on the joint angle values supplied as inputs in Simulink. When a uniform input angle of 30° is applied, the resulting gripper configuration is illustrated in Fig. 12. It was observed that all segments subtend an angle of 30° with respect to the central axis.

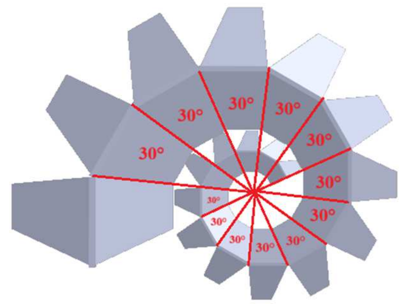

Fig. 12. Simulation of the soft gripper configuration at a uniform joint angle of 30°

C. Dynamic Analysis of Soft Gripper

In forward dynamics, the inputs to the equations of motion are the applied forces or torques, while the outputs are the resulting position, velocity, and acceleration of the system. In inverse dynamics, conversely, the inputs are the prescribed motion parameters, and the outputs are the required forces or torques necessary to achieve the desired motion.

The gripper mass was assumed to be 90 g, and the segment mass distribution ranged from 18 g at the base to 0.16 g at the tip. The TPU95A material was modeled with a density of 1210 kg/m³, a Rayleigh damping ratio of 0.15, and elasticity of 26 MPa. Gravity was applied in the negative y-direction with $g = 9.81$m/s², and the motor torque constant was set to $K_t = 0.74$ N·m/A, the radius of the pulley was 25 mm. Rayleigh damping was considered to model friction at the joints.

For the sliding mode controller, the integral gain, switching gain, and boundary layer thickness were defined as $K_i = 2$ m/s², $K_s = 20$ N, and $\phi = 0.1$ m/s, respectively.

Fig. 13 presents the trajectory defined for the dynamic analysis of the soft gripper along with the corresponding gripper configurations obtained at each time step.

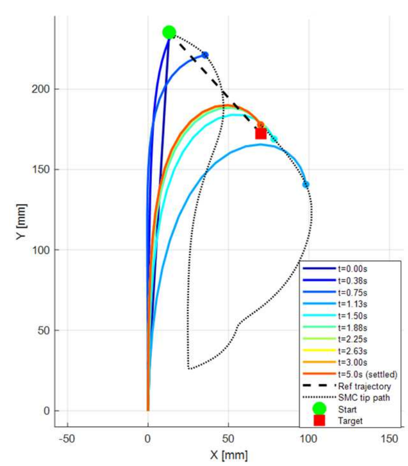

Fig. 13. Defined trajectory and corresponding soft gripper configurations.

Fig. 14 illustrates the end-effector positions along the defined trajectory, while Figs. 15 and 16 present the corresponding position errors and velocity profiles, respectively.

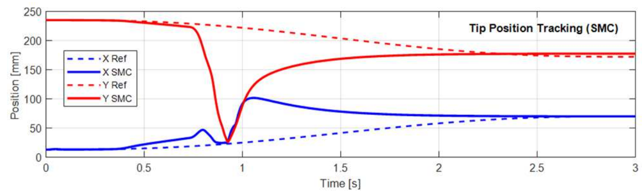

Fig. 14. End-effector positions along the defined trajectory.

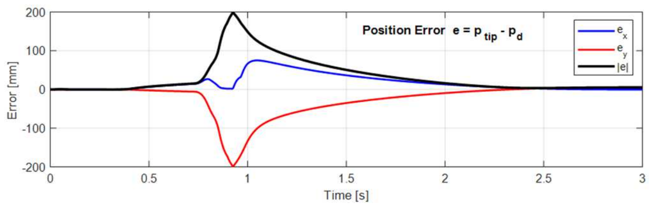

Fig. 15. Position error of end effector.

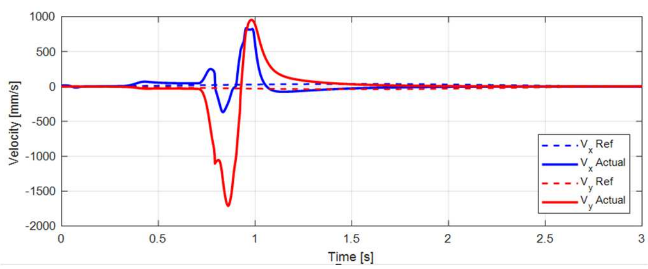

Fig. 16. Velocity of the end-effector.

IV. CONCLUSION

In this study, the design and analysis of a logarithmic spiral-shaped soft gripper were presented in detail. Forward kinematic formulations were derived and validated through simulation-based quantitative comparisons. Joint workspace characteristics and inter-joint distances were analyzed using SolidWorks and MATLAB. Furthermore, the developed model was implemented in Simscape and Simulink to investigate system constraints and joint angle limits. Dynamic analysis was performed using the Lagrange–Euler formulation, and the end-effector position and velocity responses were evaluated along a predefined trajectory. A sliding mode controller was employed for system control. Finally, an experimental setup was established to validate the theoretical findings, confirming the reliability and practical applicability of the designed gripper.

A. *Future works*

Building upon the theoretical and experimental findings of this study, the integration of the developed soft gripper into a global parallel manipulator is planned for future investigation. The incorporation of compliant structures into parallel robotic systems, which inherently exhibit limited workspace, aims to improve system efficiency and versatility across a wider range of applications.

In future work, a pick-and-place application will be investigated. Combined kinematic analyses of the rigid and soft structures will be conducted, along with the characterization of the dynamic properties of the integrated system. Furthermore, orientation and stabilization control of the gripper based on platform inclination will also be investigated.

REFERENCES

[1] C. Li, and C. D. Rahn, “Design of Continuous Backbone, Cable-Driven Robots,” Journal of mechanical design, vol. 124, pp. 265–271, 2002.

[2] W. McMahan, V. Chitrakaran, M. Csencsits, D. Dawson, and I.D. Walker “Field trials and testing of the octArm continuum manipulator,” IEEE International Conference on Robotics and Automation (ICRA), 2006.

[3] B. Mazzolai, L. Margheri, M. Cianchetti, P. Dario, and C. Laschi, “Soft-robotic arm inspired by the octopus: II. From artificial requirements to innovative technological solutions,” Bioinspiration and biomimetics, 025005, 2012.

[4] T. Deng, H. Wang, W. Chen, X. Wang, and R. Pfeifer, “Development of a new cable-driven soft robot for cardiac ablation,” IEEE International Conference on Robotics and Biomimetics (ROBIO), vol. 124, pp. 728–733, 2013.

[5] F. Renda, M. Giorelli, M. Calisti, M. Cianchetti, and C. Laschi, “Dynamic model of a multibending soft robot arm driven by cables,” IEEE Transactions on robotics, vol. 30, pp. 1109–1122, 2014.

[6] A. Firouzeh, S. Mirrazavi, A. Billard, and J. Paik, “An under actuated robotic arm with adjustable stiffness shape memory polymer joints,” IEEE International Conference on Robotics and Automation (ICRA), 2015.

[7] J. Paek, I. Cho, and J. Kim, “Microrobotic tentacles with spiral bending capability based on shape-engineered elastomeric microtubes,” Scintific reports 5, 10768, vol. 7, pp. 639–648, 2015.

[8] S. K. Mitchell, X. Wang, E. Acome, T. Martin, K. Ly, N. Kellaris, V. G. Venkata, and C. Keplinger, “An Easy-to-Implement Toolkit to Create Versatile and High-Performance HASEL Actuators for Untethered Soft Robots,” Advance science, vol. 6, 1900178, 2019.

[9] Z. Xie, A. G. Domel, N. An, C. Green, Z. Gong, T. Wang, E. M. Knubben, J. C. Weaver, K. Bertoldi, and L. Wen, “Octopus arm-inspired tapered soft actuators with suckers for improved grasping,” Soft robotics, vol. 7, pp. 639–648, 2020.

[10] Z. Zhang, X. Wang, D. Meng, and B. Liang, "Bioinspired spiral soft pneumatic acturator and its characterization," Journal of bionic enginnering, vol. 18, pp. 1101–1116, 2021.

[11] J. Zhang, Y. Hu, Y. Li, K. Ma, Y. Wei, J. Yang, Z. Wu, H. Rajabi, H. Peng, and J. Wu, “Versatile like a seahorse tail: a bio-inspired programmable continuum robot for conformal grasping,” Advanced intelligent systems, vol. 4, 2200263, 2022.

[12] I. Zournatzis, S. Kalaitzakis, and P. Polygerinos, “Softer: a spiral soft robotic ejector for sorting applications,” IEEE robotics and automation letters, vol. 8, pp. 7098–7105, 2023.

[13] I. H. Taylor, M. Bawa, and A. Rodriguez, “A tactile-enabled hybrid rigid-soft continuum manipulator for forceful enveloping grasps via scale invariant design,” IEEE International Conference on Robotics and Automation (ICRA), 2023.

[14] S. Sugiura1, J. Unde, Y. Zhu, and Y. Hasegawa, “High-strength and flexible mechanism for body weight support,” Robomech journal, vol. 40, 16, 2023.

[15] Z. Wang, N. M. Freris, X. Wei, “SpiRobs: Logarithmic spiral-shaped robots for versatile grasping across scales,” Device, vol. 3, 100646, 2025.

[16] H. Walser, “Spirals, helical lines, and spiral-like figures,” eBook, Switzerland, Springer, 2022, pp. 3–5.

[17] Z. BİNGÜL and S. KÜÇÜK, “Robot kinematiği”, Türkiye, Umuttepe yayınları, 2021, pp. 104–120.

[18] Z. BİNGÜL and S. KÜÇÜK, “Robot dinamiği ve kontrolü”, Türkiye, Umuttepe yayınları, 2017, pp. 3–22.